

# Nanosized $\text{CaCO}_3$ as Hard Template for Creation of Intracrystal Pores within Silicalite-1 Crystal<sup>†</sup>

Haibo Zhu,<sup>‡</sup> Zhicheng Liu,<sup>§</sup> Yangdong Wang,<sup>§</sup> Dejin Kong,<sup>§</sup> Xiaohong Yuan,<sup>§</sup> and Zaiku Xie<sup>\*,‡,§</sup>

School of Chemistry and Chemical Technology, Shanghai Jiao Tong University, 800 Dongchuan Road, Shanghai 200240, China, and SINOPEC Shanghai Research Institute of Petrochemical Technology, 1658 Pudong Beilu, Shanghai 201208, China

Received May 22, 2007. Revised Manuscript Received July 31, 2007

The silicalite-1 crystal with intracrystal pores in the range of 50–100 nm was synthesized by using the nanosized  $\text{CaCO}_3$  as a hard template. The nanosized  $\text{CaCO}_3$  can be trapped into the silicalite-1 crystal during the crystallization process. By means of acid dissolution, the encapsulated nanoparticles were removed, giving rise to the intracrystal pores within the zeolite crystal. Characterization techniques including XRD, TEM, SEM, and  $\text{N}_2$  adsorption provided the detailed information on this hierarchical pore structure. The hydroxyl groups on the surface of  $\text{CaCO}_3$  are essential to taking the hard template effect. The secondary pores within zeolite correspond well to the morphology of the nanosized  $\text{CaCO}_3$ , which confirms the template effect of nanosized  $\text{CaCO}_3$ . These results suggest that using  $\text{CaCO}_3$  as a hard template may be a useful approach for the synthesis of hierarchical porous materials.

## Introduction

Zeolites are the crystalline porous materials with uniform pores in the molecular dimension, as well as a high internal surface, flexible framework, and controllable chemistry, making them widely application in catalysis, purification, adsorption, separation, and other industrial fields.<sup>1</sup> But the small channels and cavities in the zeolite framework, usually in the range of 0.5–1.5 nm, not only reduce the diffusion of reagents and reaction products through the pore network but also limit the bulk molecules involved the reaction. The finding of mesoporous materials with pore sizes of 2–50 nm, such as MCM-41, MCM-48, and SBA-15, may afford an opportunity to overcome this problem.<sup>2,3</sup> However, the weak acidity and low hydrothermal stability resulting from the amorphous nature of the mesoporous walls dramatically prevent them from being used in practical applications in industrial fields.

In an attempt to circumvent such difficulty, the construction of mesopore-modified zeolites with the advantages of microporous and mesoporous materials may show satisfactory activity toward some catalytic reactions.<sup>4</sup> The template-directed method has been exploited to synthesize mesoporous zeolites. Compared to conventional steaming and chemical leaching approaches, this technique provides a route for the formation of mesopores in zeolites in a controllable manner.

Carbon-based porous materials, such as carbon black,<sup>5</sup> multiwall carbon nanotube,<sup>6</sup> and carbon nanofiber,<sup>7</sup> are effective templates for the synthesis of mesoporous zeolites. Jacobsen et al. have investigated the synthesis of mesoporous zeolites including ZSM-5, ZSM-11, TS-1, TS-2, and silicalite-2 with a pore size distribution of 10–100 nm by using carbon black and multiwall carbon nanotubes as mesopore-forming templates.<sup>8,9</sup> Tao et al. have reported the preparation of zeolite ZSM-5 and Y monolith with a bimodal pore structure of uniform mesopores by the templating method using a carbon aerogel of uniform mesopores.<sup>10–14</sup> An ordered mesoporous aluminosilicate with completely crystalline ZSM-5 wall structure has been successfully synthesized, upon the recrystallization of SBA-15 using in situ formed CMK-5 as the hard template.<sup>15</sup> The ZSM-5 zeolite with unique supermicropores has been obtained by synthesizing the zeolite using well-ordered mesoporous carbon (CMK-3) as the solid template, and the texture properties of the resulting ZSM-5 can be tailored by changing the nature of the (CMK-3) template.<sup>16</sup>

(5) Jacobsen, C. J. H.; Madsen, C.; Houzvicka, J.; Schmidt, I.; Carlsson, A. *J. Am. Chem. Soc.* **2000**, *122*, 7116.

(6) Schmidt, I.; Boisen, A.; Gustavsson, E.; Stahl, K.; Pehrson, S.; Dahl, S.; Carlsson, A.; Jacobsen, C. J. H. *Chem. Mater.* **2001**, *13*, 4416.

(7) Janssen, A. H.; Schmidt, I.; Jacobsen, C. J. H.; Koster, A. J.; de Jong, K. P. *Microporous Mesoporous Mater.* **2003**, *65*, 59.

(8) Kustova, M. Y.; Hasselriis, P.; Christensen, C. H. *Catal. Lett.* **2004**, *96*, 205.

(9) Schmidt, I.; Krogh, A.; Wienberg, K.; Carlsson, A.; Brorson, M.; Jacobsen, C. J. H. *Chem. Commun.* **2000**, 2157.

(10) Tao, Y.; Kanoh, H.; Kaneko, K. *J. Am. Chem. Soc.* **2003**, *125*, 6044.

(11) Tao, Y.; Kanoh, H.; Hanzawa, Y.; Kaneko, K. *Colloids Surf., A* **2004**, *241*, 75.

(12) Tao, Y.; Kanoh, H.; Kaneko, K. *J. Phys. Chem. B* **2003**, *107*, 10974.

(13) Li, W. C.; Lu, A. H.; Schüth, F. *Chem. Mater.* **2005**, *17*, 3620.

(14) Tao, Y.; Hattori, Y.; Matumoto, A.; Kanoh, H.; Kaneko, K. *J. Phys. Chem. B* **2005**, *109*, 194.

(15) Fang, Y. M.; Hu, H. Q. *J. Am. Chem. Soc.* **2006**, *128*, 10636.

(16) Yang, Z.; Xia, Y.; Mokaya, R. *Adv. Mater.* **2004**, *16*, 727.

<sup>†</sup> Part of the "Templated Materials Special Issue".

<sup>\*</sup> To whom correspondence should be addressed. E-mail: xzk@sript.com.cn. Fax: 86 21 68462283.

<sup>‡</sup> Shanghai Jiao Tong University.

<sup>§</sup> Shanghai Research Institute of Petrochemical Technology.

(1) Corma, A. *Chem. Rev.* **1995**, *95*, 559.

(2) Kresge, C. T.; Leonowicz, M. E.; Roth, W. J.; Vartuli, J. C.; Beck, J. S. *Nature* **1991**, *352*, 710.

(3) Zhao, D.; Feng, J.; Huo, Q.; Melosh, N.; Fredrickson, G. H.; Chmelka, B. F.; Stucky, G. D. *Science* **1998**, *279*, 548.

(4) Hartmann, M. *Angew. Chem., Int. Ed.* **2004**, *43*, 5880.

Recently, the mesoscale polymer template route has been developed to fabricate hierarchical mesoporous zeolites. The silane functionalized polyethylenimine has shown promise in the synthesis of MFI and FAU zeolites with small intracrystal mesopores and narrow pore size distribution.<sup>17</sup> Xiao et al. have demonstrated a facile, controllable, and universal route for the synthesis of hierarchical mesoporous zeolites templated from a mixture of small organic ammonium salt and mesoscale cationic polymer.<sup>18</sup> Meanwhile, the organosilane-modified surfactant designed by Choi and colleagues has been found to be effective in synthesizing polycrystalline zeolite assemblies with relatively uniform mesopores that lead to superior performance in the catalytic reactions involving large organic molecules.<sup>19–21</sup>

Herein, we describe a new method by using a hard template to synthesize silicalite-1 with intracrystal pores. The nanosized  $\text{CaCO}_3$ , which is cheap and easily available, is used as the hard template to create the intracrystal pores within zeolite crystal.

### Experimental Section

**Materials.** Hydrophilic and hydrophobic nanosized  $\text{CaCO}_3$  used as a hard template were obtained from Shanghai Yaohua nanotech Corporation (China). The particle size distribution of  $\text{CaCO}_3$  is in the range of 50–100 nm, and the surface of the hydrophobic  $\text{CaCO}_3$  is modified by fatty acid. Aerosil-200 (99%, degussa), NaOH (99%), and tetrapropyl ammonium hydroxide (25%, denoted as TPAOH) were commercial available and used in the synthesis without further purification.

**Synthesis of Silicalite-1 with Intracrystal Pores.** In a typical synthesis of hierarchical porous silicalite-1, 6 g of the nanosized  $\text{CaCO}_3$  was added to a clear solution of tetrapropylammonium hydroxide, water, and NaOH. The suspension was under strong stirring in order to produce a paste in which the nanosized  $\text{CaCO}_3$  is highly dispersed. Four grams of Aerosil-200 was then slowly added into this suspension. The resulting mixture underwent ultrasonic agitation for 10 min in order to give the homogeneous dispersion of  $\text{CaCO}_3$  particle into silica gel. Afterward, the homogeneous mixture was vigorously stirred for 2 h. The resulting mixture of silica gel (0.4TPAOH:0.03 $\text{Na}_2\text{O}$ :1 $\text{SiO}_2$ :20 $\text{H}_2\text{O}$ ) and the nanosized  $\text{CaCO}_3$  was introduced to a Teflon-lined steel autoclave for further hydrothermal treatment. The hydrothermal crystallization was carried out at 140 °C for 7 days. After the completion of the hydrothermal synthesis, the composite was acid-treated to dissolve the nanosized  $\text{CaCO}_3$ , which released the secondary pores within the crystal. The HCl solution was added to the composite dropwise until the pH value was below 6.0 and no gas came out from the product. The as-synthesized zeolite was isolated by filtration, washed with water, and dried at 100 °C for 2 h. The organic structure-directing agent trapped in the pores was thoroughly removed by calcination at 550 °C for 6 h.

For comparison, the synthesis procedure without the addition of the nanosized  $\text{CaCO}_3$  was also performed in the same condition.

**Steam Treatment.** The hydrothermal stability test was carried out by flowing water through the sample hold on a microreactor at

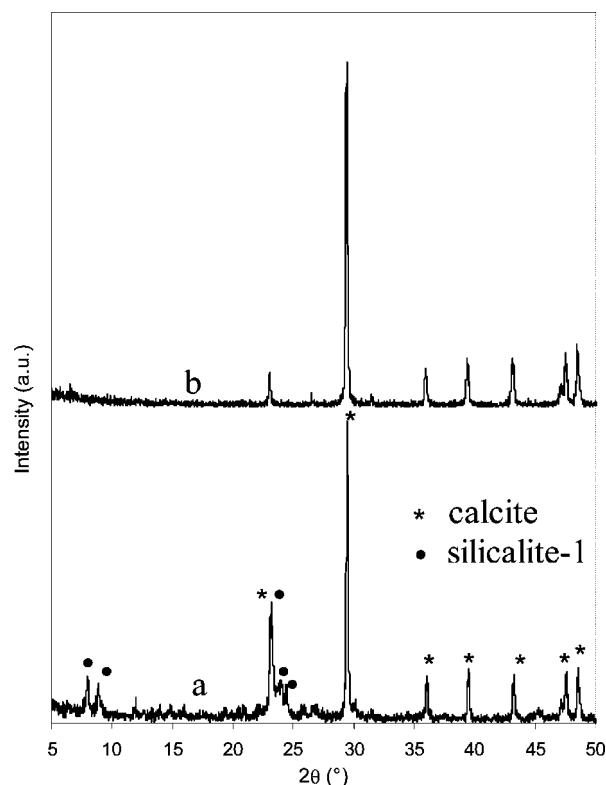


Figure 1. XRD patterns of (a) silicalite-1/ $\text{CaCO}_3$ , and (b) nanosized  $\text{CaCO}_3$ .

600 °C for 6 h, and the water flow was generated by a pump. Finally, the obtained samples were taken out and dried for XRD characterization.

**Characterization Methods.** X-ray powder diffraction (XRD) patterns were measured on a Bruker diffractometer equipped with a rotating anode and Cu KR radiation. The microstructure characterizations were carried out using a JSM-7401F scanning electron microscopy (SEM) operating at 5 kV. Transmission electron microscopy (TEM) studies were carried out on a Tecnai 20 S-TWIN instrument using an electron beam generated by a CeB6 filament and an acceleration voltage of 120 kV. Samples for TEM studies were prepared by dipping a carbon-coated copper grid into a suspension of samples in ethanol that was presonicated. Infrared spectra (IR) data was recorded on a Nicolet5700 Fourier Transform Infrared Spectrophotometer; the samples were ground with KBr and pressed into thin wafers. The nitrogen adsorption/desorption isotherms were measured at −196 °C on a Micromeritics ASAP 2020 M instrument. Before measurement, samples were evacuated overnight at 250 °C. The BET surface area was calculated from the linear part of the BET plot according to IUPAC recommendations. The mesopore size distribution was analyzed from the nitrogen desorption branch using the BJH model.

### Results and Discussion

The X-ray powder diffraction patterns of  $\text{CaCO}_3$  and the silicalite-1/ $\text{CaCO}_3$  composite are shown in Figure 1. Diffraction peaks located at  $2\theta = 23.1, 29.4, 35.9, 39.4, 43.1, 47.6$ , and  $48.5^\circ$  clearly reveal that  $\text{CaCO}_3$  belongs to the calcite phase.<sup>22</sup> The composite of silicalite-1/ $\text{CaCO}_3$  exhibits two groups of diffraction peaks. The peaks with

(17) Wang, H.; Pinnavaia, T. J. *Angew. Chem., Int. Ed.* **2006**, *45*, 7603.

(18) Xiao, F. X.; Wang, L. F.; Yin, C. Y.; Lin, K. F.; Di, Y.; Li, J. X.; Xu, R. R.; Su, D. S.; Schlögl, R.; Yokoi, T.; Tatsumi, T. *Angew. Chem., Int. Ed.* **2006**, *45*, 3090.

(19) Choi, M.; Cho, S. H.; Srivastava, R.; Venkatesan, C.; Choi, D. H.; Ryoo, R. *Nat. Mater.* **2006**, *5*, 718.

(20) Choi, M.; Srivastava, R.; Ryoo, R. *Chem. Commun.* **2006**, 4380.

(21) Srivastava, R.; Choi, M.; Ryoo, R. *Chem. Commun.* **2006**, 4489.

(22) Wang, C. Y.; Sheng, Y.; Zhao, X.; Zhao, J. Z.; Ma, X. K.; Wang, Z. C. *Mater. Sci. Eng., C* **2007**, *27*, 42.

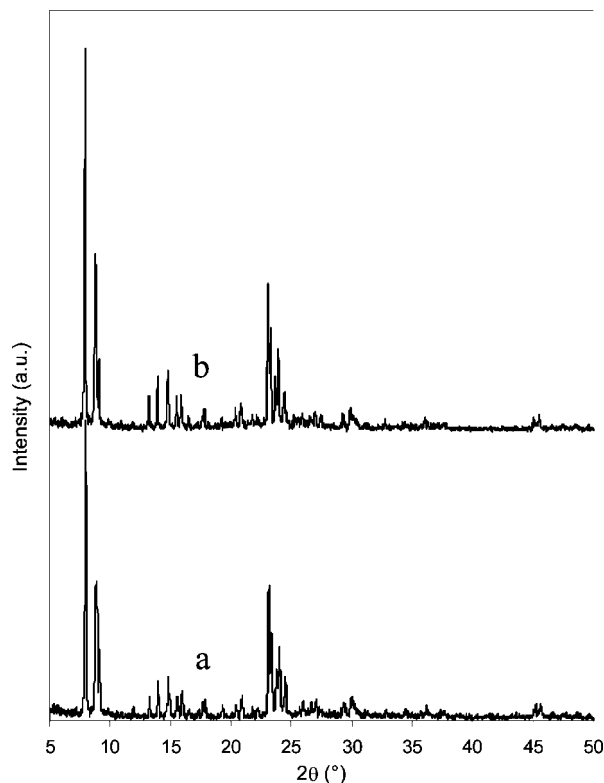


**Figure 2.** XRD patterns of (a) silicalite-1 with intracrystal pores, and (b) conventional silicalite-1.

higher intensity are ascribed to the diffraction of calcite, suggesting that  $\text{CaCO}_3$  is stable enough to resist the hydrothermal synthesis in alkaline media. In addition, the characteristic peaks of silicalite-1 emerging at  $2\theta = 7.9, 8.8, 23.1, 24.0,$  and  $24.5^\circ$  are also detectable in the composite of silicalite-1/ $\text{CaCO}_3$ .<sup>23</sup>

The comparison of X-ray powder diffraction patterns of the material obtained by the removal of  $\text{CaCO}_3$  from the silicalite-1/ $\text{CaCO}_3$  composite and the conventional silicalite-1 are shown in Figure 2. After the removal of  $\text{CaCO}_3$ , the peaks indexed to the crystalline calcite disappear completely. Determined from an EDS mounted on the SEM, the residual content of  $\text{CaCO}_3$  occluded in zeolite is only about 0.1%, which is negligible.  $\text{CaCO}_3$  is easily soluble in an acidic medium, even though the weak organic acid such as acetic acid can remove  $\text{CaCO}_3$  trapped into zeolite. For the reasons stated above, the acid treatment can dissolve the nanosized  $\text{CaCO}_3$  encapsulated in the crystal, releasing the corresponding intracrystal pores within crystal. On the other hand, the characteristic diffraction peaks of silicalite-1 become evident in the new material. This new material shows a high level of crystallinity comparable to that of the conventional silicalite-1, which is synthesized in the same conditions without the addition of nanosized  $\text{CaCO}_3$ . The comparison of X-ray powder diffraction means that the crystallinity of the last product is not remarkably influenced by the nanosized  $\text{CaCO}_3$ .

The nanosized particles play a decisive role in generating the intracrystal pores within silicalite-1, so the morphology of  $\text{CaCO}_3$  is important to evaluate the hard template effect.

The SEM images in Figure 3 give details on its morphology. The low magnification image shows that the particles are uniform. The SEM image taken at a magnification of 40000 times reveals that the particles exhibit nearly cubic shape and the particle size is in the range of 50–100 nm.

The results of scanning electron microscopy (SEM) for the hard-template-directed silicalite-1 are shown in Figure 4, and the sample appears to be highly crystalline. Estimated from the SEM overview, the average crystal size of silicalite-1 is in the range of 400–800 nm. Interestingly, some mesopores and macropores caused by the acid dissolution of  $\text{CaCO}_3$  that are opening at the external surface of the silicalite-1 can be directly observed in the high-magnification image of the SEM. Such intracrystal pores leading to the surface may promote the diffusion of bulk guest molecules into the internal surface of zeolite.

A TEM image is a projection of the mass density encountered by electrons passing through the sample; pores show up as bright areas. Therefore, it is a powerful technique for direct observation of secondary pores in zeolite.<sup>24</sup> The representative TEM images of the intracrystal-pore-modified zeolite are shown in Figure 5. The zeolite particles display regular shape in the TEM images. Hence, they should be considered as the single crystals. The TEM images under the high magnification show that the noncrystallographic pores created by the hard template are clearly visible in the images. The intracrystal pores are different from the regular mesopore structure in typical mesoporous materials and are randomly distributed in a whole crystal. It also can be observed that some noncrystallographic pores are interconnected to each other in a single crystal; accordingly, such pore system can be beneficial for efficient mass transport in zeolite crystal. Besides, the shape of the intracrystal pores is consistent with the morphology of cubic-shaped  $\text{CaCO}_3$ , suggesting that the secondary pore structure imprints the morphology of the nanosized  $\text{CaCO}_3$ . The TEM images prove that the nanosized inorganic material takes a significant template effect on creating secondary pores within zeolite crystal.

The  $\text{N}_2$  adsorption isotherm of the silicalite-1 with intracrystal pores is shown in Figure 6, and the corresponding pore size distribution is given in the inset of Figure 6. The  $\text{N}_2$  adsorption isotherm exhibits a steep increase at relatively low pressure ( $P/P_0 < 0.02$ ). This adsorption is interpreted as micropores filling and capillary condensation. Besides, the  $\text{N}_2$  isotherm shows a hysteresis loop from  $P/P_0 = 0.8$  to  $P/P_0 = 1$ . This hysteresis loop is relative to the existence of the intracrystal pores.<sup>25</sup> Relative to conventional ordered mesoporous materials, the pore size distribution of the mesopores in the silicalite-1 sample is relatively wide. The pore size distribution is calculated from the desorption branch of the isotherms on the basis of the Barrett–Joyner–Halenda (BJH) model, and the result shows that the pore width is widely distributed in the range of 50–100 nm. This result is not only in good agreement with the particle diameter of

(23) Van Koningsveld, H.; Jansen, J. C.; van Bekkum, H. *Zeolite* **1990**, *10*, 235.

(24) Boisen, A.; Schmidt, I.; Carlsson, A.; Dahl, S.; Brorson, M.; Jacobsen, C. J. H. *Chem. Commun.* **2003**, 958.

(25) Groen, J. C.; Peffer, L.; A, A.; Pérez-Ramírez, J. *Microporous Mesoporous Mater.* **2003**, *60*, 1.

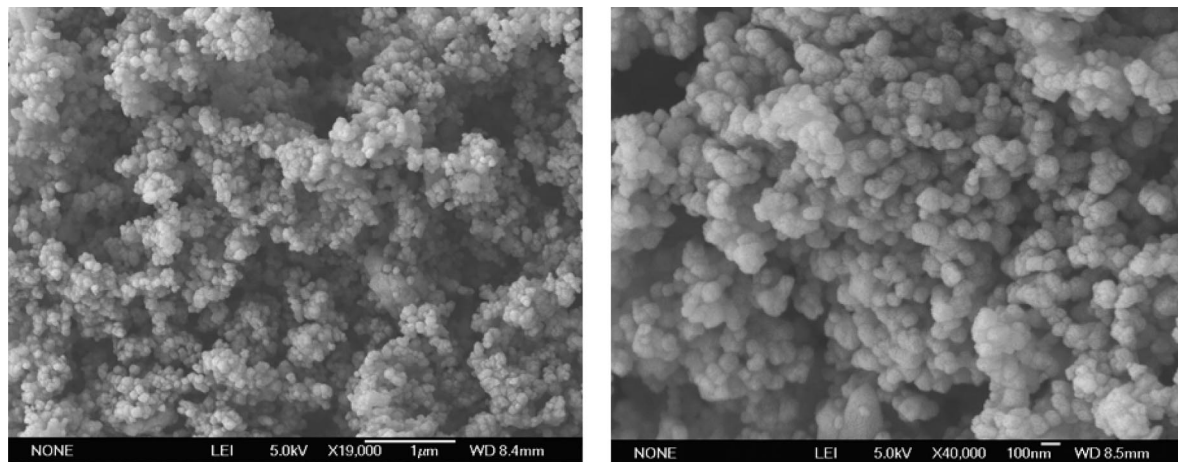


Figure 3. Low- and high-magnification SEM image of nanosized  $\text{CaCO}_3$ .

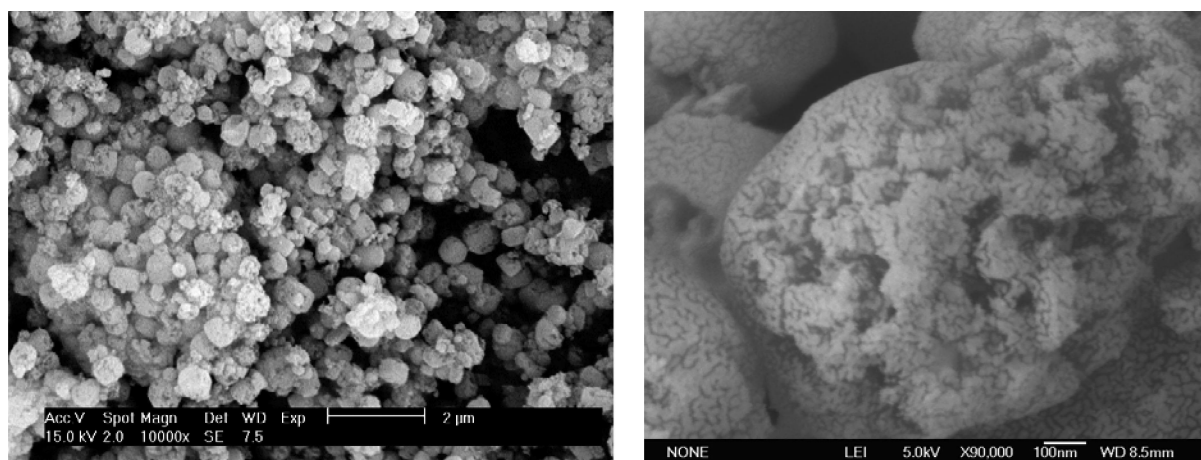


Figure 4. Low- and high-magnification SEM image of silicalite-1 with intracrystal pores.

the nanosized  $\text{CaCO}_3$  but also consistent with the pore size directly observed from the TEM image. It is important to note that the pronounced peak at 4 nm in the BJH desorption pore size distribution does not suggest real pore, which is due to the tensile strength effect (TSE) of the adsorbed phase.<sup>26</sup> Quantitatively, the BET total surface area of the sample is 445  $\text{m}^2/\text{g}$ , with micropore and mesopore areas of 215 and 230  $\text{m}^2/\text{g}$ , respectively. The total pore volume is 0.40  $\text{cm}^3/\text{g}$ , consisting of micropore volume of 0.10  $\text{cm}^3/\text{g}$  (calculated by the  $t$ -plot method of Lipens and de Boer<sup>27</sup>) and mesopore volume of 0.30  $\text{cm}^3/\text{g}$ . The micropore volume of this new material is almost same as that of the conventional silicalite-1 zeolite.<sup>28</sup> The  $\text{N}_2$  adsorption isotherm as well as the TEM image result suggest that the intracrystal pores within silicalite-1 are caused by the nanosized  $\text{CaCO}_3$  trapped into the crystal during the zeolization.

It is well-known that the drawback of mesoporous and macroporous materials is the low stability and hydrothermal stability, resulting from the amorphous wall. Many methods have been developed to enhance the ability to resist the hydrothermal condition, but most of them are far from

industrial requirements.<sup>29–31</sup> To evaluate the hydrothermal stability of this material, we put the sample under steam destruction at 600  $^\circ\text{C}$  for 6 h. The comparison of XRD patterns of the parent sample and the sample treated by steam (see the Supporting Information), indicates that the sample retains the crystallinity at a high level even after steam treatment for a long time. Meanwhile, the intracrystal pores can be also observed in the TEM image. It can thus be concluded that steam treatment at high temperature does not cause significant destruction on its structure. Although the intracrystal pores are introduced into the crystal through  $\text{CaCO}_3$  template, the atom distribution in zeolite still retains a short-range order. The hydrothermal stability can be attributed to the highly ordered crystalline structure.

The creation of hierarchal pores in silicalite-1 is attributed to the use of nanosized  $\text{CaCO}_3$  as a hard template. The efficiency of the hard template effect largely depends on the surface property of nanosized  $\text{CaCO}_3$ . Hydrophilic and hydrophobic  $\text{CaCO}_3$  have been used to conduct the synthesis in the same condition. These two types of nanosized  $\text{CaCO}_3$  are the same in morphology but different in surface properties. The hydrophobic  $\text{CaCO}_3$  is produced upon the modi-

(26) Groen, J. C.; Pérez-Ramírez, J. *Appl. Catal., A* **2004**, 268, 121.

(27) Lipens, B. C.; de Boer, J. H. *J. Catal.* **1965**, 4, 319.

(28) Li, W. C.; Lu, A. H.; Palkovits, R.; Schmidt, W.; Spliethoff, B.; Schüth, F. *J. Am. Chem. Soc.* **2005**, 127, 12595.

(29) Selvaraj, M.; Kawi, S. *Chem. Mater.* **2007**, 19, 509.

(30) Kato, M.; Shigeno, T.; Kimura, T.; Kuroda, K. *Chem. Mater.* **2005**, 17, 6416.

(31) Kruk, M.; Celer, E. B.; Jaroniec, M. *Chem. Mater.* **2004**, 16, 698.

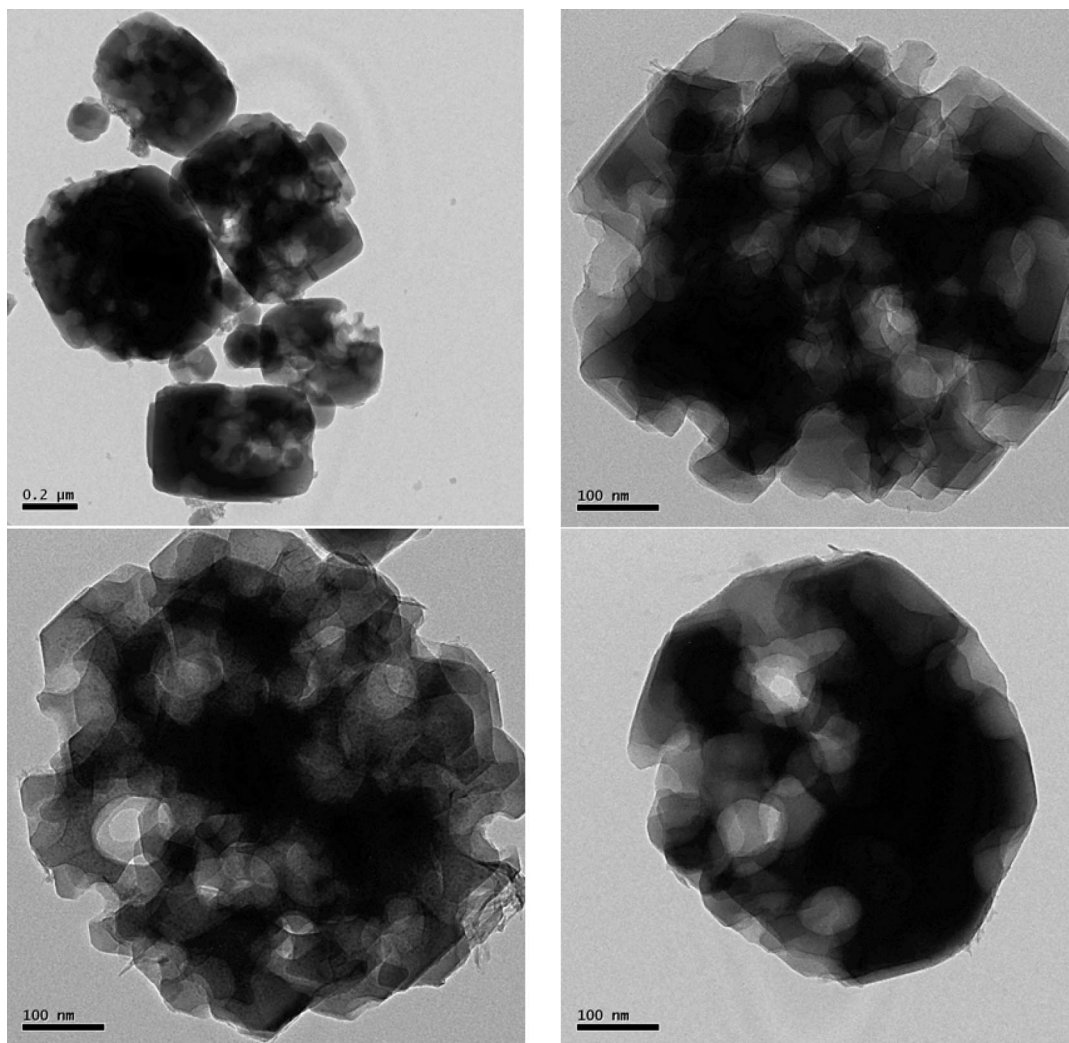


Figure 5. TEM images of silicalite-1 synthesized in the presence of the nanosized  $\text{CaCO}_3$ .

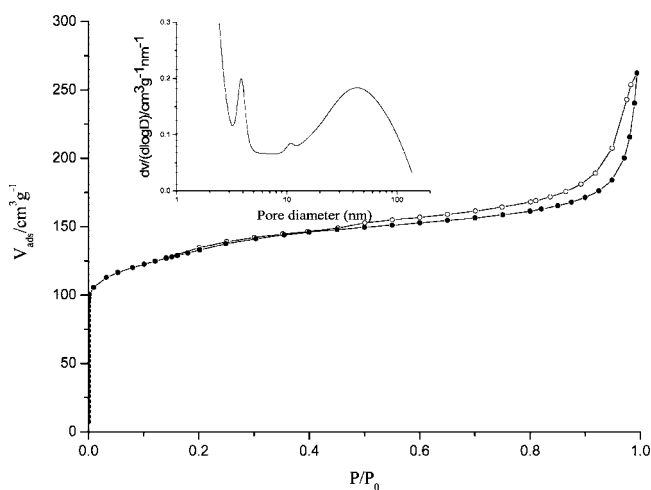


Figure 6.  $\text{N}_2$  adsorption/desorption isotherm of silicalite-1 samples with intracrystal pores, and mesopore size distributions calculated from the adsorption branch by the BJH method.

fication of the surface of hydrophilic  $\text{CaCO}_3$  by fatty acid. In addition to the vibration modes assigned to calcite structure absorption, the absorption occurring around 2927 and 2865  $\text{cm}^{-1}$  are detected in the IR of hydrophobic  $\text{CaCO}_3$  (see the Supporting Information). They are due to the characteristic absorption of H—C—H asymmetric and sym-

metric stretching vibrations, respectively, which result from the alkyl groups in the fatty acid. The IR data prove that the organic moieties are bound onto the surface of hydrophobic  $\text{CaCO}_3$ . Because of the difference in surface properties, only the hydrophilic nanosized  $\text{CaCO}_3$  can work well to yield the intracrystal pores in silicalite-1 crystal. In the case of the synthesis using hydrophobic  $\text{CaCO}_3$  as a template, the last product is the conventional zeolite without the hierarchical pore.

The hard template effect of the nanosized  $\text{CaCO}_3$  may be related to its hydrophilic property. This effect is different from the synthesis of mesoporous zeolite templated by carbon-based porous materials in the previous reports.<sup>5,6</sup> Because of the pores in carbon materials, the zeolite crystal growth proceeds within the void; subsequently, large zeolite single crystal grows and encapsulates the whole carbon particles. On the contrary,  $\text{CaCO}_3$  is a solid rather than porous material. However, there is a large number of hydroxyl groups on the surface of the hydrophilic nanosized  $\text{CaCO}_3$ . These highly active hydroxyl groups can give rise to strong interaction between  $\text{SiO}_2$  and  $\text{CaCO}_3$ . Because of this interaction, the nanosized  $\text{CaCO}_3$  dispersed in the silica gel is encapsulated into the crystal during the crystallization process. Because of the attachment of fatty acid to the surface

of hydrophilic  $\text{CaCO}_3$ , the active hydroxyl groups may be protected. Therefore, it hinders the interaction between  $\text{SiO}_2$  and  $\text{CaCO}_3$ . This phenomenon proves that the hydrophilic property of the nanosized  $\text{CaCO}_3$  is essential to taking the template effect.

### Conclusions

In conclusion, the preparation of silicalite-1 single crystal with intracrystal pores in the range of 50–100 nm by using the nanosized  $\text{CaCO}_3$  as a hard template is reported for the first time. The nanosized  $\text{CaCO}_3$  can be trapped in the silicalite-1 crystal during the crystallization process. By means of acid dissolution, the encapsulated nanoparticles are removed and give rise to the intracrystal pores within the zeolite crystal. The hydroxyl groups on the surface of  $\text{CaCO}_3$  are essential to taking the hard template effect. The combined use of X-ray diffraction, TEM, SEM image analysis, and  $\text{N}_2$  adsorption/desorption proves that the synthesized material exhibits two levels of hierarchy in pore organization. The intracrystal pores correspond well to the morphology of the nanosized  $\text{CaCO}_3$ , which confirms the effectiveness of

nanosized  $\text{CaCO}_3$  as a hard template in the creation of secondary pores within zeolite.

Hierarchical zeolites combining an intrinsic micropore with an intracrystal mesopore and macropore system has shown unique properties in catalysis and other fields.<sup>32–34</sup> Detailed studies of the synthesis, characterization, and catalytic reactivity of such porous zeolites are currently underway.

**Acknowledgment.** We gratefully acknowledge financial support from the Major State Basic Research Development Program of the People's Republic of China (2003CB615802).

**Supporting Information Available:** XRD patterns and IR spectra (PDF). This material is available free of charge via the Internet at <http://pubs.acs.org>.

CM071385O

- 
- (32) Christensen, C. H.; Schmidt, I.; Carlsson, A.; Johannsen, K.; Herbst, K. *J. Am. Chem. Soc.* **2005**, *127*, 8098.
- (33) Christensen, C. H.; Johannsen, K.; Schmidt, I.; Christensen, C. H. *J. Am. Chem. Soc.* **2003**, *125*, 13370.
- (34) Schmidt, I.; Krogh, A.; Wienberg, K.; Carlsson, A.; Brorson, M.; Jacobsen, C. J. H. *Chem. Commun.* **2000**, 2157.